

The Problem Parameters Effects on Transient Behavior of MHD Duct Flow

Elif EBREN KAYA*¹, Münevver TEZER-SEZGİN²

¹The Scientific and Technological Research Council of Turkey, 06680, Ankara, Turkey

²Middle East Technical University, Faculty of Arts and Science, Department of Mathematics, 06800, Ankara, Turkey

(Alınış / Received: 15.02.2022, Kabul / Accepted: 03.04.2023, Online Yayınlanma / Published Online: 25.08.2023)

Keywords

Drbem,
Unsteady Mhd flow,
Time-dependent magnetic
field

Abstract: The present study focuses the effects of Reynolds number R_e and magnetic Reynolds number R_m on the transient behavior of the MHD flow. The incompressible, electrically conducting and viscous fluid flows through a long pipe subjected to magnetic field $B_0(t)=B_0f(t)$. B_0 is the intensity and $f(t)$ is the time varying function of the magnetic field which is chosen as polynomial, trigonometric, exponential and logarithmic function to illustrate the problem parameters effects. The R_e and R_m effects on the behavior of the flow at transient levels are studied with these functions by taking Hartmann number Ha value as 20. The unsteady MHD equations in coupled form are treated by using the dual reciprocity boundary element method (DRBEM). The study reveals that, when R_e or R_m increases the time level where the flow elongates is postponed to a further time level. Moreover, the increase in R_e flattens the flow as in the increase of Hartmann number. However, the increase in R_m increases the flow magnitude. The transient flow and induced current contours are demonstrated for several R_e and R_m values. After the flow elongates, the flow and induced current lines preserve the behavior for polynomial, exponential and logarithmic type $f(t)$ while trigonometric type $f(t)$ causes the flow to show periodic behavior.

Problem Parametrelerinin MHD Kanal Akışının Zamana Bağlı Davranışına Etkileri

Anahtar Kelimeler

Drbem,
Mhd akış,
Zamana bağlı manyetik alan

Öz: Bu çalışma, problem parametreleri olarak ifade edilen Reynolds R_e ve manyetik Reynolds R_m sayılarının zamana bağımlı MHD akış üzerindeki etkilerini incelemektedir. Dışarıdan uygulanan manyetik alan etkisiyle akan sıvı viskoz, sıkıştırılmaz ve elektriği iletmektedir. Bu manyetik alan $B_0(t)=B_0f(t)$ ile gösterilmiştir. Eşitlikteki B_0 manyetik alan şiddeti ve $f(t)$ ise zamana bağlı bir fonksiyondur. Çalışmada $f(t)$ fonksiyonu polinom, üstel, logaritmik ve trigonometrik fonksiyonlar tipinde seçilip problem parametrelerinin akış davranışına etkileri farklı zaman seviyelerinde sunulmuştur. Kupule olarak bulunan MHD akış denklemleri, kanal kesitinde karşılıklı sınır elemanı metodu kullanılarak çözülmüştür. R_e veya R_m sayılarındaki artışın akış elongasyonunu daha ileri bir zaman seviyesine ötelediği görülmüştür. Ayrıca, R_m sayısı büyürken akışın şiddetinin büyüdüğü fakat R_e sayısı büyürken akışın düzleştiği görülmüştür. Polinom, üstel ve logaritmik tipinde seçilen $f(t)$ fonksiyonları için akış elongasyonu gerçekleştikten sonra, akış ve indüklenen akım bütün farklı R_e ve R_m sayıları için aynı davranışı göstermiştir. Fakat trigonometrik fonksiyon tipinde seçilen $f(t)$ fonksiyonu akış elongasyonunun belirli bir süreyle yinelenmesini sağlamıştır.

1. Introduction

The magnetohydrodynamic (MHD) duct flows have important applications in different branches of engineering, science and biology as electrolytes, blood flow measurements, MHD generators, etc. Considering the fluid mechanics and electrodynamics

equations together, the analytical solution to the MHD flow is inaccessible except the special cases (i.e. insulated or conducting duct walls) and simple geometry of the flow region. Therefore, some numerical approaches are developed for an approximate solution of MHD flow problems. The steady MHD flow through a channel having different

wall conductivities has been studied by using the constant and linear BEMs in [1]. The steady MHD flow equations have been treated by finite element method (FEM) in terms of velocity and induced current profiles in [2]. A solution for convection-diffusion type equations in coupled form has been derived in [3] and it is used to solve MHD flow problems with different wall conductivities. Finite volume method (FVM) and spectral element technique have been implemented to solve unsteady MHD flow problems in [4]. The numerical solutions have been conducted for several Hartmann number values with different wall conductivities and the magnetic field has different orientations. In all above mentioned studies, the concern is to use different numerical methods to achieve more accurate results, however, the use of uniform applied magnetic field for Re and Rm as 1 is in common. Then, time-dependent applied magnetic field is introduced in [5]. Then, Bandaru, et al. [6] have used the procedure of finite difference in time-boundary element in space for their solution of unsteady MHD flow. Previously, we have concentrated on the influence applied magnetic field depending on time, $B_0(t)=B_0f(t)$, on the flow behavior by taking several definitions of time-varied function $f(t)$, but by setting $Re = Rm = 1$ in [7]. It has been seen that for each considered function $f(t)$, the flow elongates at a certain time level which becomes earlier with an increased value of Ha .

In this paper, the problem parameters Re and Rm effects on the the transient MHD flow behavior has been examined. The fully-developed, laminar, unsteady MHD flow is studied under influence time dependent applied magnetic field $B_0(t)=B_0f(t)$. The fluid flowing through square duct is incompressible, viscous and electrically conducting. The MHD flow equations are treated with DRBEM iteratively. The main advantage of DRBEM is to obtain both unknown velocity and induced current at once by only discretizing the boundary of duct. The flow and induced current configurations are simulated with various values of Re as 5, 10, 25 and Rm as 1, 3, 5 along with polynomial, trigonometric, logarithmic and exponential function $f(t)$. The transient behavior of the flow has been revealed that, the flow elongation starts at a further time level with the increase in Re or Rm values. Although, both Re and Rm are in front of the time derivative terms of the flow equations, Re effect on flow is more dominant than Rm due to the fluid electrical conductivity present in Rm . For the trigonometric type $f(t)$, the same period in the flow is seen at a further time level for all values of Re and Rm as in the case of $Re = Rm = 1$ [7].

2. Material and Method

2.1. Mathematical formulation

We consider the unsteady MHD flow in a long pipe of

square cross-section (duct). Fluid velocity is parallel to the axis of the pipe (z -axis), and the externally applied magnetic field depending on time, $B_0(t)=B_0f(t)$ is in the x -direction. B_0 is the intensity of applied magnetic field at the initial time. The flow is fully-developed, and the velocity and the induced magnetic field have only pipe-axis direction components, i.e. $\vec{V}=(0,0,V_z(x,y,t))$ and $\vec{B}=(B_0f(t),0,B_z(x,y,t))$. Thus, the equations of motion (for an incompressible, viscous fluid) and the magnetic induction equations become

$$\mu \nabla^2 V_z + B_0 f(t) \frac{1}{\mu e} \frac{\partial B_z}{\partial x} = \frac{\partial P}{\partial z} \tag{1}$$

$$\eta \nabla^2 B_z + B_0 f(t) \frac{\partial V_z}{\partial x} = 0 \tag{2}$$

where μ , μe , and σ are the coefficient of viscosity, magnetic permeability and electrical conductivity, respectively. $\eta=(\sigma \mu e)^{-1}$ is the magnetic diffusivity. The function $f(t)$ describes the profile of the applied magnetic field depending on time.

Introducing dimensionless variables

$V=\frac{1}{V_0}V_z$, $B=\frac{1}{V_0 \mu e}(\sigma \mu)^{-1/2} B_z$, $x'=\frac{x}{L_0}$, $y'=\frac{y}{L_0}$ where $V_0=-(L_0)^2 \frac{\partial P}{\partial z} / \mu$ is the characteristic (mean-axis) velocity and L_0 is the characteristic length and $\frac{\partial P}{\partial z}$ is the pressure gradient.

The governing non-dimensional equations then (dropping prime notation)

$$\Delta V + \bar{M} \frac{\partial B}{\partial x} = -1 + Re \frac{\partial V}{\partial t} \tag{3}$$

$$\Delta B + \bar{M} \frac{\partial V}{\partial x} = Rm \frac{\partial B}{\partial t} \tag{4}$$

where $\bar{M}=Ha f(t)$ and $Ha=B_0 L_0 \sqrt{\sigma/\mu}$ is the Hartmann number. The non-dimensional parameters $Re= L_0 V_0 / \mu$, $Rm= \sigma L_0 V_0 \mu e$ are the Reynolds and magnetic Reynolds numbers, respectively.

The duct $\Omega=[-1,1] \times [-1,1]$ walls have the no-slip velocity and they are insulated, i.e.

$$V(x, y, t) = 0, B(x, y, t) = 0, t > 0 \tag{5}$$

zero initial values for the velocity and the induced magnetic field are taken

$$V(x, y, 0) = 0, B(x, y, 0) = 0 \quad (x, y) \in \Omega. \tag{6}$$

These MHD flow equations (3)-(4) are coupled in terms of the velocity V and the induced magnetic field B due to the time derivative terms. Thus, they have to be solved as a whole.

2.2. Application of the Drbem

The coupled MHD flow equations in (3)-(4) are rewritten to leave the Laplacian terms alone

$$\Delta V = -1 + Re \frac{\partial V}{\partial t} - \bar{M} \frac{\partial B}{\partial x} \quad (7)$$

$$\Delta B = Rm \frac{\partial B}{\partial t} - \bar{M} \frac{\partial V}{\partial x} \quad (8)$$

in $\Omega \times [0, \infty)$.

Then, the DRBEM procedure can be used with the fundamental solution of Laplace's equation $u^* = \frac{\ln(1/r)}{2\pi}$ given in [8]. The weighted residual statement is obtained after applying Green's second identity twice as

$$c_i V_i + \int_{\Gamma} q^* V d\Gamma - \int_{\Gamma} u^* \frac{\partial V}{\partial n} d\Gamma = - \int_{\Omega} \left(-1 + Re \frac{\partial V}{\partial t} - \bar{M} \frac{\partial B}{\partial x} \right) u^* d\Omega \quad (9)$$

$$c_i B_i + \int_{\Gamma} q^* B d\Gamma - \int_{\Gamma} u^* \frac{\partial B}{\partial n} d\Gamma = - \int_{\Omega} \left(Rm \frac{\partial B}{\partial t} - \bar{M} \frac{\partial V}{\partial x} \right) u^* d\Omega \quad (10)$$

where q^* stands for normal derivative of u^* as $\frac{\partial u^*}{\partial n}$. The coefficient c_i is either 0.5 or 1 depending the source point i is on the boundary or inside the region Ω , respectively. $i=1, \dots, N$, N denotes the number of constant boundary elements.

The integrands of the domain integrals are considered as inhomogeneities. These inhomogeneous terms are expanded as

$$b_1(x, y) = \left(-1 + Re \frac{\partial V}{\partial t} - \bar{M} \frac{\partial B}{\partial x} \right) = \sum_{j=1}^{N+L} \alpha_j f_j(x, y) \quad (11)$$

$$b_2(x, y) = \left(Rm \frac{\partial B}{\partial t} - \bar{M} \frac{\partial V}{\partial x} \right) = \sum_{j=1}^{N+L} \beta_j f_j(x, y) \quad (12)$$

where $f_j(x, y)$'s are the radial basis functions which are connected to \hat{u}_j through $\nabla^2 \hat{u}_j = f_{j=1+r_{ij}}$, the unknown coefficients α_j 's and β_j 's are undetermined constants. r_{ij} denotes distance between the points i

and j where $i, j = 1, \dots, N+L$. f_j is assumed to be varying linearly.

Substituting $f_j = \nabla^2 \hat{u}_j$ into the equations (11)-(12) and then applying Green's second identity twice result in

$$c_i V_i + \int_{\Gamma} q^* V d\Gamma - \int_{\Gamma} u^* \frac{\partial V}{\partial n} d\Gamma = \sum_{j=1}^{N+L} \alpha_j \left(c_i \hat{u}_{ij} + \int_{\Gamma} q^* \hat{u}_j d\Gamma - \int_{\Gamma} u^* \hat{q}_j d\Gamma \right) \quad (13)$$

$$c_i B_i + \int_{\Gamma} q^* B d\Gamma - \int_{\Gamma} u^* \frac{\partial B}{\partial n} d\Gamma = \sum_{j=1}^{N+L} \alpha_j \left(c_i \hat{u}_{ij} + \int_{\Gamma} q^* \hat{u}_j d\Gamma - \int_{\Gamma} u^* \hat{q}_j d\Gamma \right) \quad (14)$$

where $\hat{q}_j = \frac{\partial \hat{u}_j}{\partial n}$.

Taking the vectors \hat{u}_j , \hat{q}_j and f_j as columns, respectively, one can construct the $(N+L) \times (N+L)$ matrices \hat{U} , \hat{Q} and coordinate matrix F . Collocating the functions $b_1(x, y)$ and $b_2(x, y)$ at $N+L$ points gives \mathbf{b}_1 , \mathbf{b}_2 vectors and two sets of linear equations as $\mathbf{b}_1 = \mathbf{F}\alpha$, $\mathbf{b}_2 = \mathbf{F}\beta$. Thus, the following matrix-vector form equations emerged as

$$\mathbf{H}\mathbf{V} - \mathbf{G} \frac{\partial \mathbf{V}}{\partial n} = (\mathbf{H}\hat{U} - \mathbf{G}\hat{Q}) \mathbf{F}^{-1} \left\{ -\mathbf{1} + Re \frac{\partial \mathbf{V}}{\partial t} - \bar{M} \frac{\partial \mathbf{B}}{\partial x} \right\} \quad (15)$$

$$\mathbf{H}\mathbf{B} - \mathbf{G} \frac{\partial \mathbf{B}}{\partial n} = (\mathbf{H}\hat{U} - \mathbf{G}\hat{Q}) \mathbf{F}^{-1} \left\{ Rm \frac{\partial \mathbf{B}}{\partial t} - \bar{M} \frac{\partial \mathbf{V}}{\partial x} \right\} \quad (16)$$

where \mathbf{V} and \mathbf{B} , $\frac{\partial \mathbf{V}}{\partial n}$ and $\frac{\partial \mathbf{B}}{\partial n}$, $\mathbf{1}$, $\frac{\partial \mathbf{V}}{\partial t}$ and $\frac{\partial \mathbf{B}}{\partial t}$ are $(N+L) \times 1$ vectors.

The entries of the enlarged \mathbf{H} and \mathbf{G} matrices are given as [8]

$$H_{ij} = c_i \delta_{ij} + \frac{1}{2\pi} \int_{\Gamma_j} \frac{\partial}{\partial n} \ln(1/r) d\Gamma_j$$

$$H_{ii} = - \sum_{j=1, j \neq i}^N H_{ij}$$

$$G_{ij} = \frac{1}{2\pi} \int_{\Gamma_j} \ln(1/r) d\Gamma_j$$

$$G_{ii} = \frac{l}{2\pi} \left(\ln \left(\frac{2}{l} \right) + 1 \right) \quad (17)$$

where δ_{ij} is Kronecker delta function and l denotes elements length.

The coordinate derivatives of \mathbf{V} and \mathbf{B} with respect to x are approximated as

$$\frac{\partial \mathbf{V}}{\partial x} = \frac{\partial \mathbf{F}}{\partial x} \mathbf{F}^{-1} \mathbf{V} \quad \text{and} \quad \frac{\partial \mathbf{B}}{\partial x} = \frac{\partial \mathbf{F}}{\partial x} \mathbf{F}^{-1} \mathbf{B}. \quad (18)$$

Euler's method is used to approximate the time derivatives in (15)-(16) as

$$\frac{\partial V}{\partial t} = \frac{V^{n+1} - V^n}{\Delta t} \quad \text{and} \quad \frac{\partial B}{\partial t} = \frac{B^{n+1} - B^n}{\Delta t} \quad (19)$$

where Δt and n are the time increment and iteration level, respectively.

Then, the equations in (15)-(16) are written for an increasing time levels as

$$\left(H - K \frac{Re}{\Delta t} \right) V^{n+1} - G \frac{\partial V^{n+1}}{\partial n} + K \left(\bar{M} \frac{\partial F}{\partial x} F^{-1} B^{n+1} \right) = K \left(-1 - \frac{Re}{\Delta t} V^n \right) \quad (20)$$

$$\left(H - K \frac{Rm}{\Delta t} \right) B^{n+1} - G \frac{\partial B^{n+1}}{\partial n} + K \left(\bar{M} \frac{\partial F}{\partial x} F^{-1} V^{n+1} \right) = K \left(-\frac{Rm}{\Delta t} B^n \right) \quad (21)$$

where matrix K denotes $(H \hat{U} - G \hat{Q}) F^{-1}$.

The equations (20)-(21) are rearranged for obtaining the solution vectors V^{n+1} , B^{n+1} , iteratively

$$H1 V^{n+1} - G \frac{\partial V^{n+1}}{\partial n} + R B^{n+1} = b_1 \quad (22)$$

$$H2 B^{n+1} - G \frac{\partial B^{n+1}}{\partial n} + R V^{n+1} = b_2 \quad (23)$$

where $H1 = H - K \frac{Re}{\Delta t}$, $H2 = H - K \frac{Rm}{\Delta t}$, $R = K \left(\bar{M} \frac{\partial F}{\partial x} F^{-1} \right)$, $b_1 = K \left(-1 - \frac{Re}{\Delta t} V^n \right)$ and $b_2 = K \left(-\frac{Rm}{\Delta t} B^n \right)$.

The matrix-vector equations (22)-(23) are solved together in coupled form by constructing the following large system as

$$\begin{bmatrix} H1 & R \\ R & H2 \end{bmatrix} \begin{bmatrix} V^{n+1} \\ B^{n+1} \end{bmatrix} = \begin{bmatrix} G & 0 \\ 0 & G \end{bmatrix} \begin{bmatrix} \frac{\partial V^{n+1}}{\partial n} \\ \frac{\partial B^{n+1}}{\partial n} \end{bmatrix} + \begin{bmatrix} b_1 \\ b_2 \end{bmatrix} \quad (24)$$

where $H1, H2, R$ and G are $(N+L) \times (N+L)$ matrices. 0 denotes zero matrix with size $(N+L) \times (N+L)$. Shuffled for obtaining the unknown entries of V, B and $\frac{\partial V}{\partial n}, \frac{\partial B}{\partial n}$ vectors inside the region and on the boundary of the duct, respectively. The shuffled equations are solved iteratively starting from zero initials.

The matrix-vector system must be solved at once for obtaining unknowns V and B values. That means, the enlarged system can not be tranformed into decoupled form as in the study [7] since there are Re and Rm coefficients different from 1 in front of the time derivatives of V and B . Thus, the equations must be solved in coupled form.

3. Results

$N=200$ constant boundary elements and $L=2500$ interior nodes are used to discretize the cross-section of the pipe $\Omega=[-1,1] \times [-1,1]$. Using polynomial, exponential, logarithmic and trigonometric function $f(t)$, the velocity and induced current values are obtained at transient time levels for $Ha=20$. The computations are carried with $\Delta t = 0.01$. The velocity and induced current profiles in pipe-axis direction are simulated at transient time levels to observe the effect of Re and Rm . The flow behavior is examined for the increase in the values of Rm as 1,3,5 when $Re=1$ in Figure 1. The applied magnetic field varies exponentially in time, i.e $f(t)=e^t$. Figure 1 shows the time levels t_n where the flow elongates (central vortex turns to be aligned parallel to the applied magnetic field direction) for each value of Rm . Actually, the flow elongates at $t_n=0.10,0.15,0.19$ for $Rm=1, 3$ and 5 , respectively. One can deduce from Figure 1 that, as Rm increases the elongation time level is postponed to an increasing time level and also the magnitude of the flow increases as the value of Rm increases. The effect of increasing Rm ($Rm \neq 1$) is seen after the elongation, that is, the flow circulates in front of the Hartmann walls and then settles down parallel to the applied magnetic field direction with a drop in its magnitude.

Figure 2 represents the flow behavior as Re values increasing for the time-varied function $f(t)=e^t$. The Reynolds number values are taken as $Re=5,10,25$ for $Rm=1$. The flow behaviors are presented at different time levels t_n where the flow elongates for the first time as well as the time levels before and after the elongations for the increase in Re values. The time levels $t_n=0.20,0.30,0.50$ are the values where the flow elongates for $Re=5,10$ and 25 , respectively. The increase in Re postpones the elongation of the flow to a further time level. Moreover, as Re increases the magnitude of the flow decreases which is an opposite effect on the behavior when it is compared with the increase in Rm .

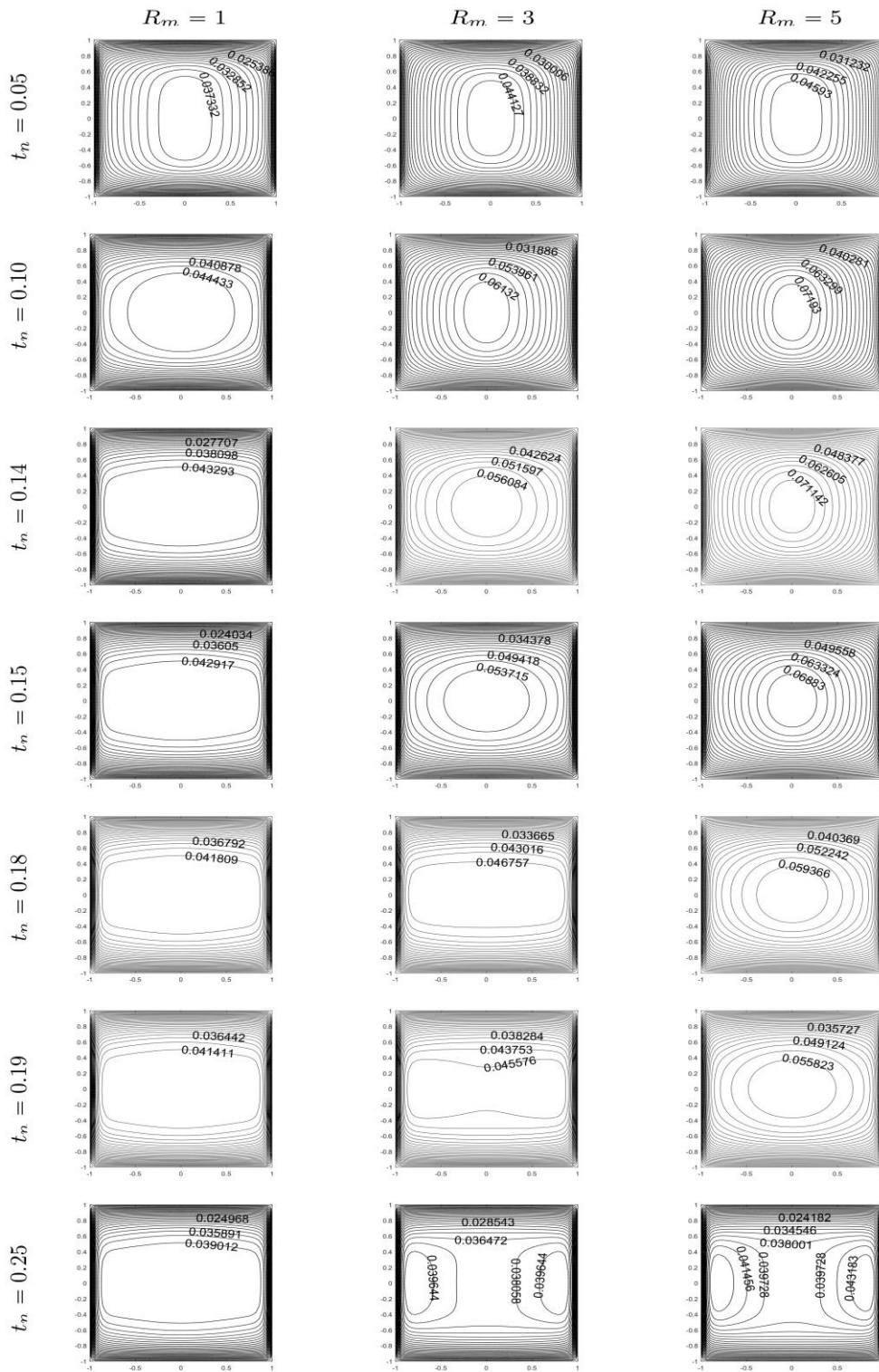


Figure 1. Velocity contours, $f(t) = e^{-t}$, $Re=1$, $R_m=1,3,5$, $Ha=20$.

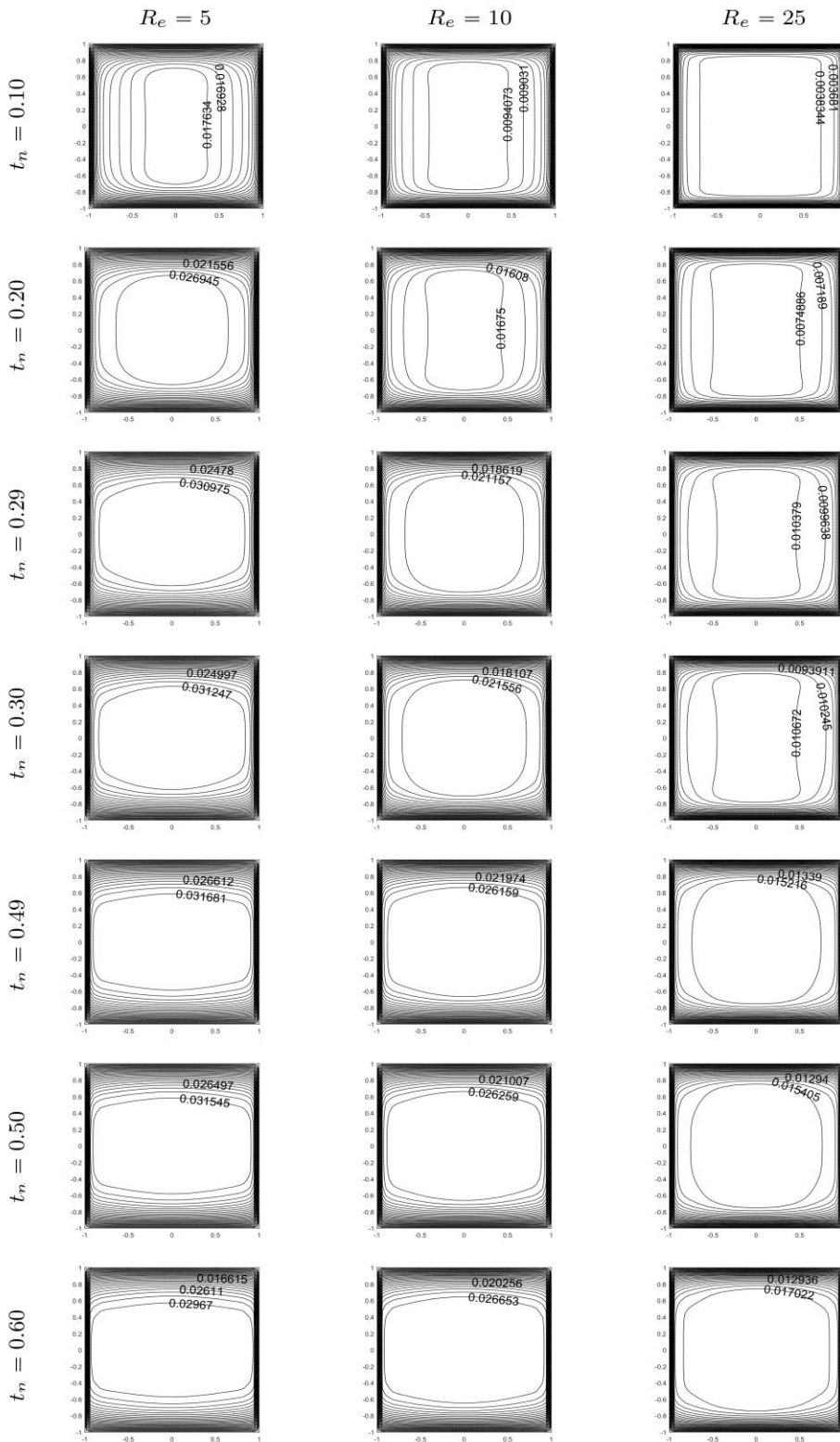


Figure 2. Velocity contours, $f(t)=e^t$, $R_m=1$, $Re=5,10,25$, $Ha=20$.

Figure 3 depicts the velocity and induced current behavior for the applied magnetic field varying linearly and exponentially in time ($f(t)=1+t$ and $f(t)=e^t$) with the increase in R_m values as 1,3,5 and $Re=1$ at the elongation time levels. The first row in Figure 3 where $Re=R_m=1$ shows an agreement with decoupled MHD equations which is possible only for

$Re=R_m=1$, [7]. The flow elongates almost at the same time levels for both linear and exponential functions for the same Re and R_m values. Although, the behavior of the induced current does not change when R_m increases, its magnitude increases as well as the increase in the flow magnitude.

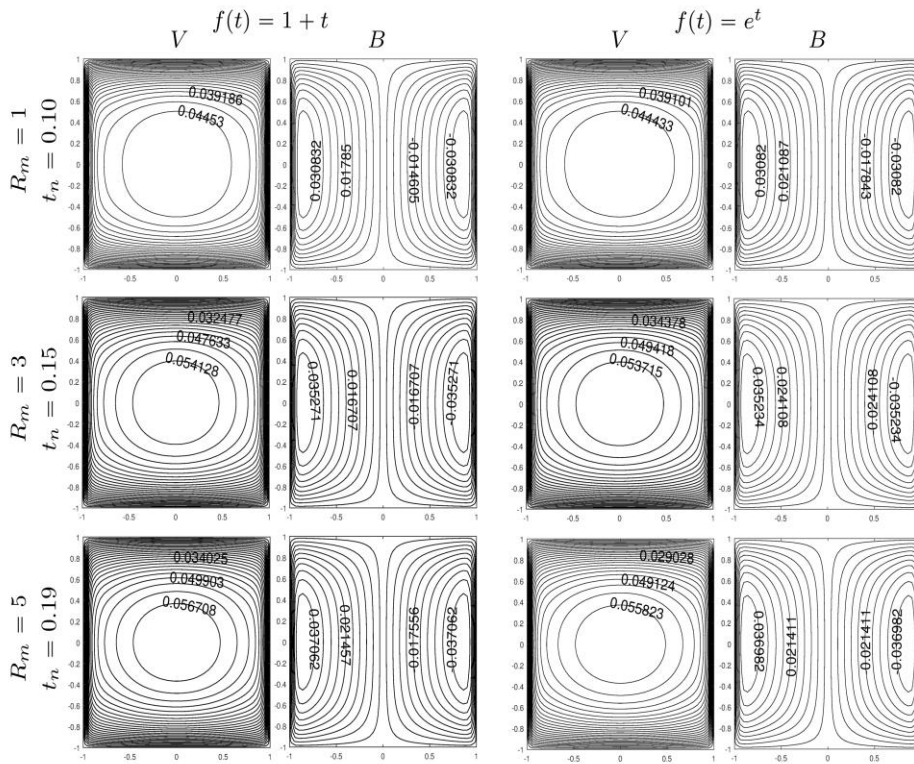


Figure 3. V, B contours, $Re=1$, $Ha=20$.

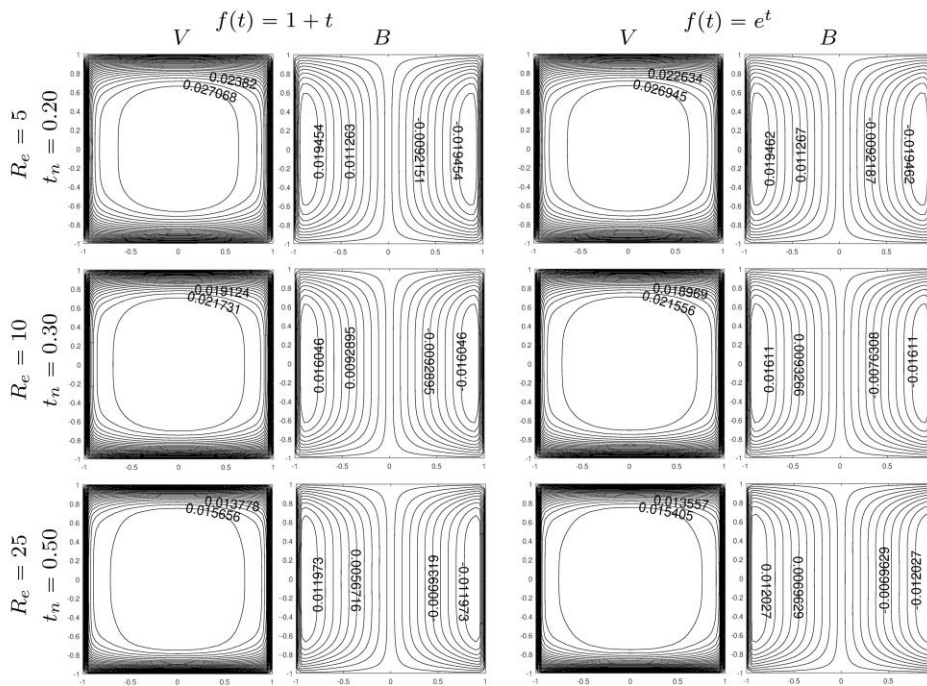


Figure 4. V, B contours, $R_m=1$, $Ha=20$.

Figure 4 shows the flow and induced current profiles for $f(t)=1+t$ and $f(t)=e^t$, keeping $R_m=1$ and for the increase in Re values as 5,10 and 25. As Re increases the induced current magnitudes decrease similar to the decrease in the flow magnitudes.

In Figure 5, the Re and R_m values are taken different than one as $Re=10$, $R_m=2$. It can be seen that, the flow

elongation occurs at $t_n=0.40$ for $Re=10$ and $R_m=2$ which is a postponed time level, with the effect of the increase in R_m , compared to the case $Re=10$ and $R_m=1$ given in Figure 4. Since the elongation occurs around small time levels (e.g. $t_n=0.40$) the effects of the functions $f(t)=1+t$, $f(t)=e^t$ are almost the same. They may differ for larger values of t but the behavior of the flows do not change after the elongations.

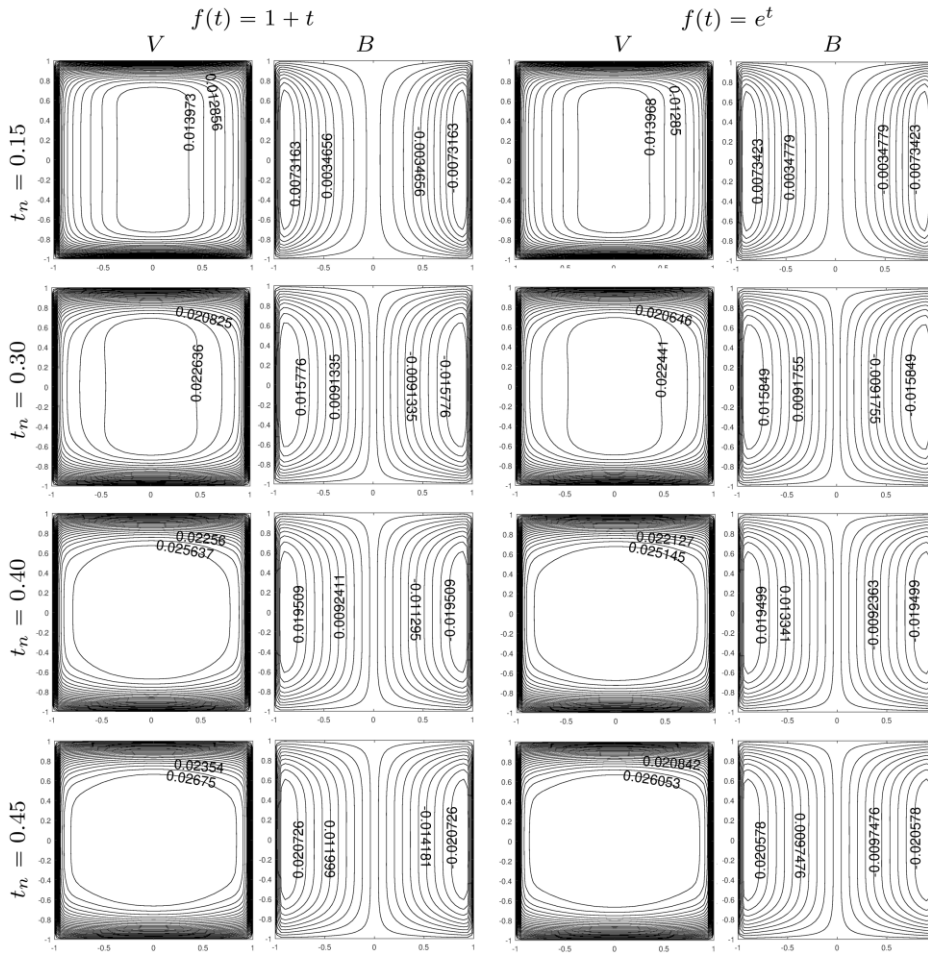


Figure 5. V, B contours, $Re=10, R_m=2, Ha=20$.

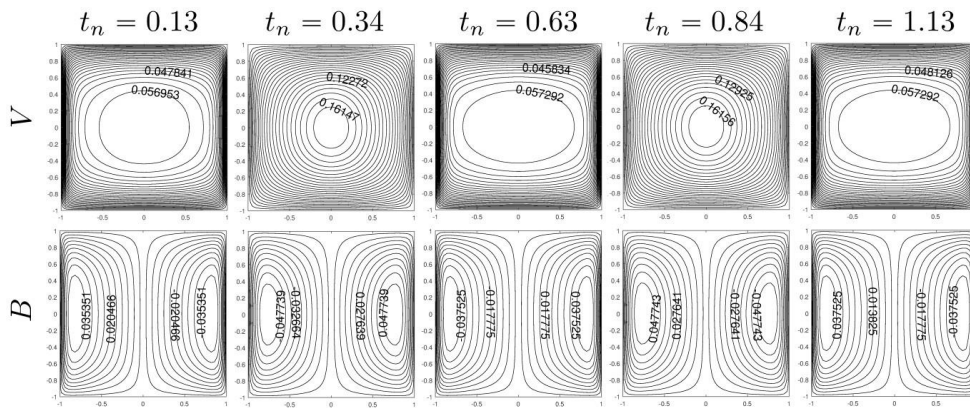


Figure 6. V, B contours, $f(t)=\cos(2\pi t), Re=R_m=1, Ha=20$.

Figure 6 stands to validate again our solution of the coupled MHD flow equations for $Re=R_m=1$ with $f(t)=\cos(2\pi t)$, with the solution in [7] obtained from the decoupled MHD equations. The period of the flow is again seen as 0.5. Then, Figure 7 depicts the profiles of the velocity and induced current for $Re=1, R_m=2$ and $Re=5, R_m=1$, respectively. In both cases, the first time level exhibits elongation of the flow for the first time. Once more, the elongation time level is postponed when compared to Figure 6. The period of

$f(t)=\cos(2\pi t)$ does not change with the changes in the values of Re and R_m staying again 0.5.

The flow and induced current profiles are demonstrated at further transient time levels for $f(t)=\cos(2\pi t)$, when $Re=5$ and $R_m=2$ in Figure 8. It is confirmed that the period of the flow for the elongation is really 0.5. The periodic effect of $f(t)$ can be seen on the flow behavior in Figures 6-8 as the flow is repeating itself.

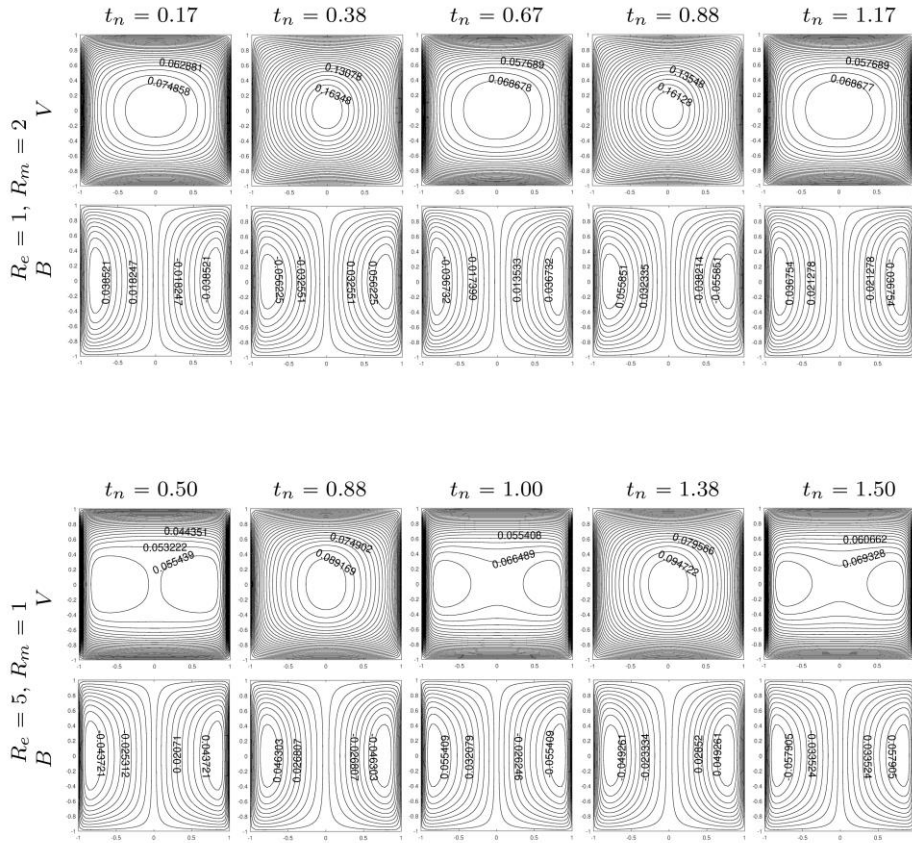


Figure 7. V, B contours for $f(t) = \cos(2\pi t)$, $Ha=20$.

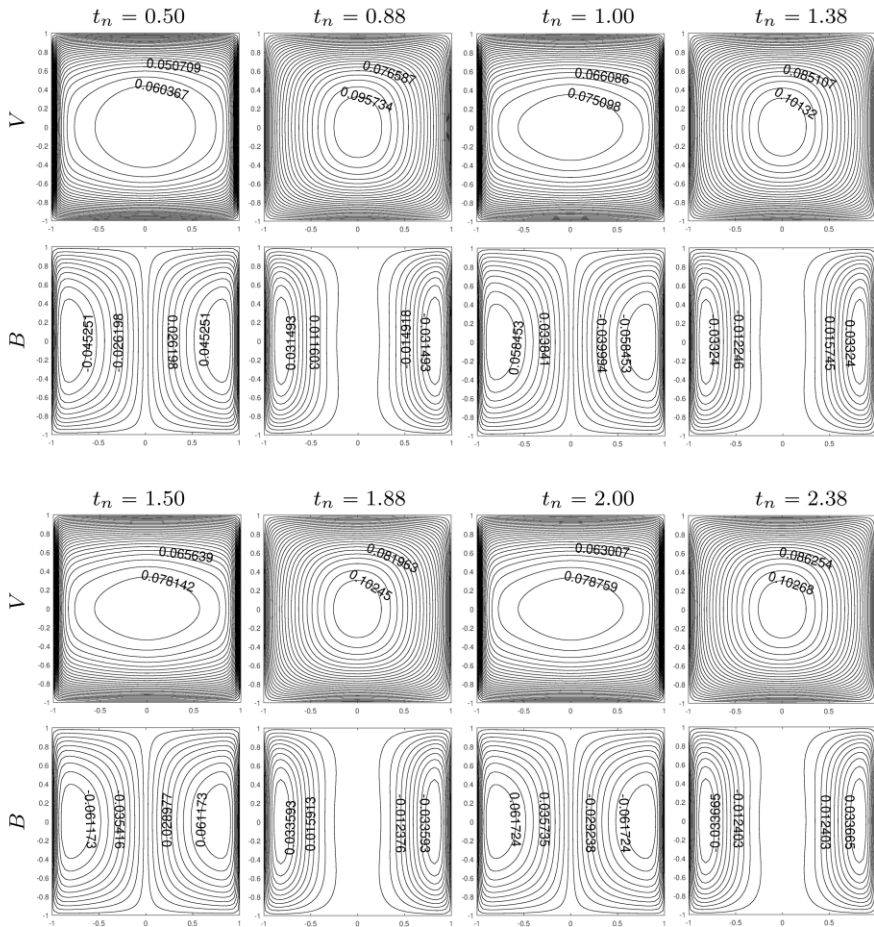


Figure 8. V, B contours for $f(t) = \cos(2\pi t)$, $Re=5$, $Rm=2$, $Ha=20$.

Figure 9 represents the flow behavior at different time levels for a time-varied function $f(t)=1+\ln(1+t)$ which is not considered in study [7]. The flow elongates at $t_n=0.11, 0.15, 0.33$ for $R_e=1=R_m$, $R_e=1$, $R_m=3$, and $R_e=10$, $R_m=1$, respectively, for this type of function. Either increasing the value of R_e or R_m postpones the time level where the flow elongates to a further time level. The velocity contours are

examined before and after the elongation time levels for comparison. It is seen that, the flow elongates at a certain time level t_n and after the elongation the Hartmann layers start to be formed. That is, a common behavior of the flow is observed for the time-varied functions $f(t)=1+t$, $f(t)=e^t$ and $f(t)=1+\ln(1+t)$.

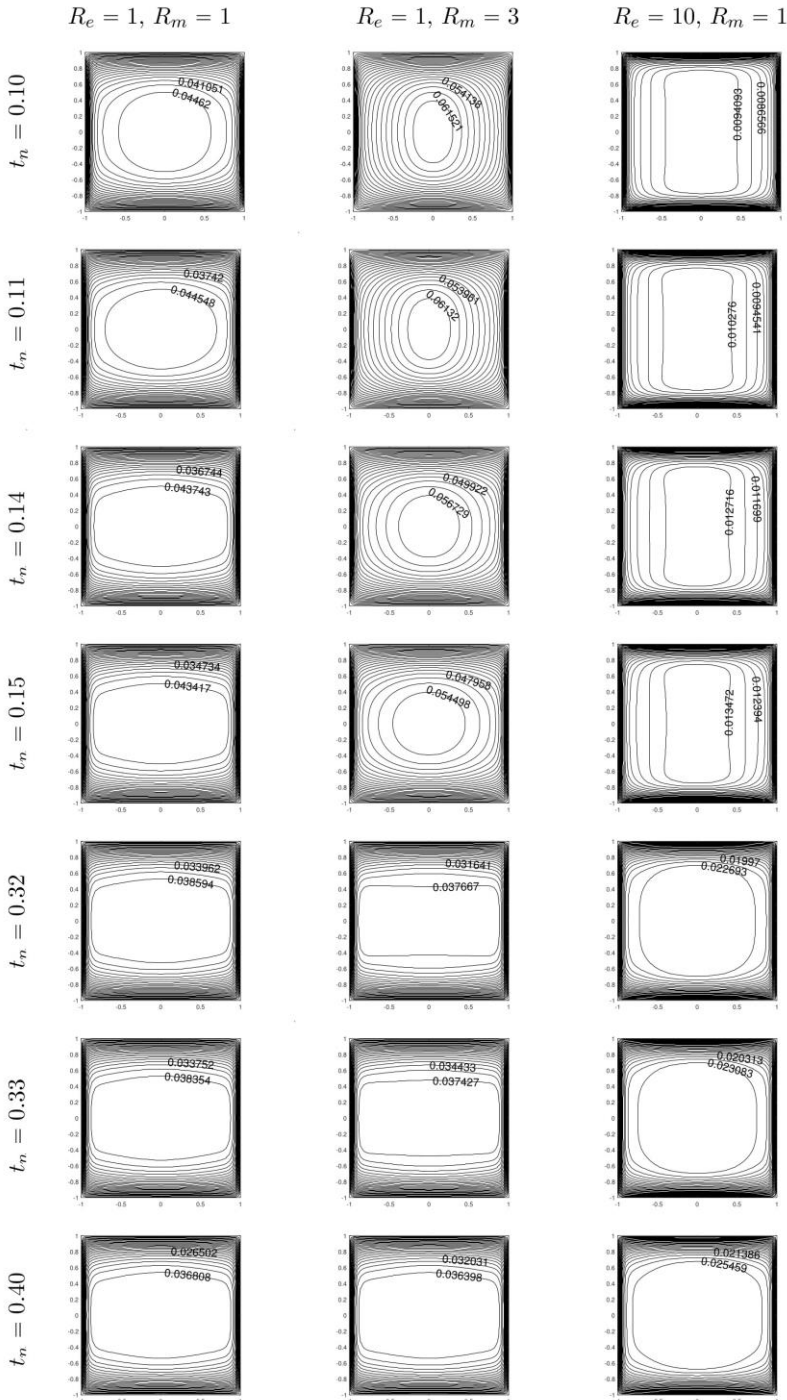


Figure 9. Velocity contours, $f(t)= 1+\ln(1+t)$, $Ha=20$.

4. Discussions and Conclusions

The unsteady MHD duct flow behavior controlled by a time dependent magnetic field $B_0(t)=B_0f(t)$ is investigated. The problem parameters, R_e and R_m

effects on the flow are examined for a fixed Hartmann number value as 20 by taking R_e as 5,10,25 and R_m as 1,3,5. The velocity and induced current profiles are visualized using polynomial, exponential, logarithmic and trigonometric types time-varied function $f(t)$.

The study reveals that, when R_m increases the flow magnitude increases up to the time level where the flow elongates, however, as R_e increases the flow magnitude decreases. The increases in R_e and R_m postpone the elliptical elongation of the flow to further time levels which are observed as a common behavior of the flow for each type function considered.

Acknowledgement

This study is obtained from Elif Ebrin Kaya's Ph.D. Thesis titled "Bem Solutions of Magnetohydrodynamic Flow Equations under Time and Axially Dependent Magnetic Field" dated September 6, 2021. The supervisor of the thesis is Prof. Dr. Münevver Tezer.

Declaration of Ethical Code

In this study, we undertake that all the rules required to be followed within the scope of the "Higher Education Institutions Scientific Research and Publication Ethics Directive" are complied with, and that none of the actions stated under the heading "Actions Against Scientific Research and Publication Ethics" are not carried out.

References

- [1] Hosseinzadeh, H., Dehghan, M., Mirzaei, D. 2013. The boundary elements method for magnetohydrodynamic (MHD) channel flows at high Hartmann numbers. *Applied Mathematical Modelling*, 37, 2337-2351.
- [2] Tezer-Sezgin, M., Köksal, S. 1989. Finite Element Method for Solving MHD Flow in a Rectangular Duct. *International Journal for Numerical Methods in Engineering*, 28(2), 445-459.
- [3] Bozkaya, C., Tezer-Sezgin, M. 2007. Fundamental Solution for Coupled Magnetohydrodynamic Flow Equations. *Journal of Computational and Applied Mathematics*, 203(1), 125-144.
- [4] Shakeri, F., Dehghan, M. 2011. A Finite Volume Spectral Element Method for Solving Magnetohydrodynamic (MHD) Equations. *Applied Numerical Mathematics*, 61(1), 1-23.
- [5] Bandaru, V. 2015. Magnetohydrodynamic duct and channel flows at finite magnetic reynolds numbers, Fakultät für Maschinenbau der Technischen Universität Ilmenau, Doctoral Thesis, Germany.
- [6] Bandaru, V., Boeck, T., Krasnov, D., Schumacher, J. 2016. A Hybrid Finite Difference-Boundary Element Procedure for the Simulation of Turbulent MHD Duct Flow at Finite Magnetic Reynolds Number. *Journal of Computational Physics*, 304, 320-339.
- [7] Ebrin Kaya, E., Tezer-Sezgin, M. 2020. DRBEM Solution of MHD Flow in a Rectangular Duct with Time-varied External Magnetic Field. *Engineering Analysis with Boundary Elements* 117, 242-250.
- [8] Partridge, P. W., Brebbia, C. A., Wrobel, L. C. 1992. *The Dual Reciprocity Boundary Element Method*, Computational Mechanics Publications, Southampton, Boston.